Tuijin Jishu/Journal of Propulsion Technology
ISSN: 1001-4055
Vol. 44 No. 4 (2023)

# Optimal Scheduling of Renewable Sources Based Micro grid with PV and Battery Storage Using Giant Trevally Optimizer

**[1]Subrat Bhol, [2]Nakul Charan Sahu, [3]Subash Ranjan Kabat**

[1]Research Scholar, Department of Electrical Engineering
ITER, Siksha'o' Anusandhan University,
Bhubaneswar, Odisha, India.
[2]Associate professor, Department of Electrical Engineering
ITER, Siksha 'o' Anusandhan University
Bhubaneswar, Odisha, India.
[3]Associate Professor, Department of Electrical Engineering
Radhakrishna Institute of Technology and Engineering, Bhubaneswar, Odisha, India

**Abstract:** This paper proposes a Giant trevally optimizer (GTO) for the optimal scheduling of a hybrid power system. This hybrid power system encompasses multiple renewable energy sources, including photovoltaic (PV) panels, wind turbines (WT), fuel cells (FC), micro turbines (MT), and a battery energy storage system (BESS). The primary objective of this method is to minimize the overall operating cost of a grid-connected micro grid while enhancing the accuracy and efficiency of the energy management system. GTO method is used to analyses the generation, storage, and response load options in order to resolve the economic dispatch difficulties. To manage with the optimal energy management of the grid connected micro grid with a high degree of uncertainties, a GTO algorithm is employed. Subsequently, the performance of this proposed technique is assessed using the MATLAB Simulink platform and compared against several existing methodologies. Notably, the proposed method yields a cost value of 270, which is notably lower than the costs associated with other existing approaches.
**Keywords:** Electromechanical, Renewable Sources, Charging, Hydrogen storage, Integrated energy system (IES), Integrated demand response, Energy management

## 1. Introduction

The 21st century still faces severe sustainability difficulties related to environmental issues and energy security [1]. Despite ongoing efforts to transition towards cleaner energy sources, most of the energy in the planet still comes from fossil fuels, which causes rising environmental damage and resource shortages. Consequently, there is a growing emphasis on exploring alternative clean energy sources with minimal environmental impact for the century ahead. Distributed energy resources (DER) are also becoming more widely recognized as beneficial alternatives as a result of the growing prices of energy derived from fossil fuels and technological improvements [2]. Sustainable energy is defined as energy produced from unconventional sources and regenerated constantly by natural processes [3]. Which significantly improve the quality and flexibility of power networks [4-6]. However, there are a number of issues that must be taken into consideration while managing distributed generation (DG) in the power system [7].

Rapid development in renewable energy technology, notably in wind and solar energy, has been seen in recent years, offering low-carbon alternatives for energy supply [8]. However, there is a chance that energy inefficiency and limited economic gains might result from uncertainty related to renewable energy sources and the independence of energy networks. The "energy internet" idea has surfaced in the energy industry as a solution to these problems [9–10]. Utilizing energy cogeneration, conversion, and storage technology, the energy internet enables the integrated functioning of gas, electricity, and heating systems, maximizing the use of renewable energy [11]. The transmission, conversion, and supply of energy are made possible by this integrated energy system (IES), which runs as a physical network under the control of an information system [12]. To address the various energy requirements of users in certain locations, such as office buildings or blocks, utilizing electrical devices, Regional Integrated Energy Systems (RIES) are implemented in metropolitan areas on the

power load side and encompass several square kilometers. 13]. Micro grids are significant RIES types that can advance energy efficiency and stability of development. [14].

There is considerable potential to influence the economics of the power generating process in order to obtain the most cost-effective distribution of energy [15–16]. The Economic Load Dispatch (ELD) problem has emerged as a significant and challenging optimization problem in the power network as a result of the sharp rise in fuel costs. When there are energy requirements that need to be brought into balance with real physical constraints and time optimization, traditional computational methods are made unable to meet the requirements because they are not smooth and convex. This situation makes the application of the model difficult and requires an effective IES model used in demand and thermal comfort. Even though optimization requires the ability to detect the worst-case scenario, the solution is frequently conservative since it prevents the worst-case scenario from occurring.[18]. Another idea is based on hybrid scenario/interval/variable data decision-making techniques to ensure that the plant operates well at load with less uncertainty in the cost of electrical and electronic connections. However, the quality of the image creation and retouching process positively affects the optimization of this process [19-20].

These are the research's primary contributions,

- The research paper's contribution is the Giant Trevally Optimizer (GTO) algorithm, which it suggests be used to optimize Scheduling micro grids with renewable source and battery storage systems.
- The integration of battery storage systems with the micro grid is also taken into account in this work. The battery's charging and discharging are taken into consideration during schedule optimization to maximize the use of stored energy.
- The paper describes the application of the GTO algorithm for improving the micro grid's scheduling.
- The paper shows the performance assessment of the suggested strategy. It contrasts the outcomes of the GTO algorithm with those of other optimization techniques frequently employed in micro grid scheduling.
- The paper include the convergence speed of the GTO algorithm, solution quality, calculation efficiency, etc. proves its superiority in many respects.
- Overall, the contribution of this research paper lies in its novel use the GTO algorithm for optimizing the scheduling of a micro grid with renewable source and battery storage systems.

The paper is structured as follows: Section 2 reviews recent literature, Section 3 explains the configuration of micro grid configuration with renewable sources and battery storage, Section 4 details the proposed technique, Section 5 presents simulation results, and Section 6 concludes the study.

## 2. Recent research works: A Brief Review

Optimal Programming of Hybrid Power Systems of employing a variety of methodologies and factors has been the subject of several research papers in the literature. Some of them have received reviews.

Eskandari *et al.* [21] have introduced a unique random structure to efficiently manage energy in micro grids that include storage, Proton exchange membrane fuel cells (PEMFC-CHP), RERs, and PHEVs. In order to account for their uncertainty, PHEV and Monte Carlo simulation (MCS) is used with the RER model, the hydrogen storage mechanism of a PEMFC-CHP unit was identified in this work. In addition, complex payment methods were used to pay for plug-in hybrid vehicles. The purpose of business objective was to increase business profit. Wang *et al.* [22] have presented challenges arising from variable renewable energy sources, This research employs an optimization routing model based on chance-constrained programming (CCP) that considers charging characteristics as well as integrated electricity-heat response to demand., and a ladder-style carbon pricing mechanism into account was harnessed to bolster system flexibility and facilitate the seamless integration of diverse energy sources. Additionally, the study evaluates potential synergies between electric-heat flexible loads and micro-energy grids through integrated demand response (IDR) strategies. Furthermore, the model incorporates a ladder-type carbon trading mechanism aimed at curbing system carbon emissions. This holistic approach aims to enhance energy system efficiency and sustainability while mitigating the uncertainties associated with renewable energy sources. Li *et al*. [23] have designed in the within the backdrop of renewable

energy's ongoing evolution, the optimal distribution model based on limited period position was adopted to determine charging characteristics, responses to electricity and electricity needs, and increase carbon pricing. Interactions between electro thermal flexible loads and micro power grids are evaluated using Integrated Demand Response (IDR). The CCP model was later simplified into a solvable mixed integer linear programming (MILP) model with parallel operations (SOT).

Alabi *et al*. [24] have demonstrated a deep learning approach and optimization model for ZCMES virtual power plants day-ahead scheduling optimization. In order to lessen the carbon emissions produced by certain machinery, a Carbon capture and storage system (CCS) was technically designed. Flexibility of electric cars was taken into account, and a clean energy marketer (CEM) strategy was developed to ensure system sustainability. Following that, situations were created utilizing the fast forward reduction approach, and scenes were then compressed using an auto encoder (AE). The best solutions were then selected using a robust-stochastic modeling method. Dey *et al*. [25] have developed an IHES based on underground space; an effective scheduling method based on deep deterministic policy gradients (DDPG) was given. A Markov decision-making process was used to frame the energy management problem to show the relationship between environmental conditions and policy. It was able to approximate deterministic policy and actor-value function. using the actor-critic structure and DDPG theory. UHS and other power conversion devices performance may be adaptively optimized by using actor-critic network training and policy iteration, which were driven by real-time response data rather than genuine system models. Zakernezhad *et al*. [26] have introduced, an active distribution system was a two-level optimization process was utilized. The distribution system operator aids the electricity market, plug-in hybrid electric vehicle lot aggregators in and demand response aggregators by providing energy and associated services. The zonal tie-line switches of a switching system can also be utilised in an active distribution system. mechanism to decrease the effects of contingencies. The architecture created to simulate active distribution systems' arbitrage approach, as well as that of demand response aggregators in real-time and day-ahead markets, was the study's main contribution. Yang *et al*. [27] have presented a carbon capture device, and a ladder-style carbon trading mechanism was made possible by an ideal scheduling model that takes demand response of cooling, heating, and electrical load into consideration. CPLEX used the objective purpose that minimizes the total of the costs associated with purchasing energy, maintaining it, emitting carbon dioxide into the atmosphere, and compensating for those costs to solve the problem as a mixed integer linear problem.

### 2.1. Background of the Research work

Recent research studies reviewed indicate that the Optimal Scheduling of Modern energy management is greatly aided by hybrid power systems. Recently, there has been a lot of emphasis on improving the effectiveness of active distribution systems while taking into account the unpredictability present in electricity production from renewable resources. For this to happen, a multi-objective optimization approach was employed. The main goals of this strategy were to reduce overall active power losses, optimize active power outputs, reduce operating expenses, and eliminate voltage variations. This optimization approach made use of a multi-objective evolutionary algorithm that included a simulated annealing algorithm. In response to this limitation, a novel framework was developed to simulate various aspects of energy management, incorporating day-ahead and in-progress preventative steps, in addition to pre- and post-event remedial activities for unforeseen circumstances. The three-stage framework was designed to address these aspects comprehensively. In the first stage, robust optimization techniques were applied to determine optimal day-ahead scheduling. Subsequently, the second stage saw a change in emphasis to the best real-time market scheduling. Finally, the third stage took into account different contingent conditions. However, one notable gap in this approach was the absence of consideration for the arbitrage process of distributed energy resource aggregators. It's important to highlight that while these methods showed promise, they were primarily suitable for discrete control of micro grids. Implementing them in more complex and larger energy systems could potentially lead to challenging high-dimensional problems that need careful consideration. This investigation was motivated by the shortcomings listed above.

## 3. Configuration of Renewable Sources Based Micro Grid with Battery Storage System

Configuration of renewable sources based micro grid with battery storage System is shown in fig 1. PV wind turbines, FC, MT, batteries, and loads connected to the utility grid make up a renewable energy source.

The primary inverter of the recommended hybrid power system (HPS) connects two buses. HPS has various power generating sources for both the DC bus and the AC bus to make up for the strength and weakness of each component. The DC bus is connected to the PV system via a boost converter, which increases the PV output voltage to that level. The windmill and DC bus are connected via a rectifier. In order to create hydrogen, which the fuel cell uses, the electrolyzer needs extra electricity. As a result, the electrolyzer serves as an energy storage device. The HPS, which is connected to the AC bus via back-to-back AC/DC and DC/AC converters, operates the MT as a standby source. A bidirectional buck/boost converter connects the battery—the HPS's emergency power source—to the DC bus. When a battery is needed, it performs admirably at modest, constant power levels. The GTO algorithm is employed to address economic dispatch problems, enabling the assessment of generation, storage, and responsive load offers. It is utilized for optimal energy management in grid-connected micro grids, particularly when dealing with a significant level of uncertainty.

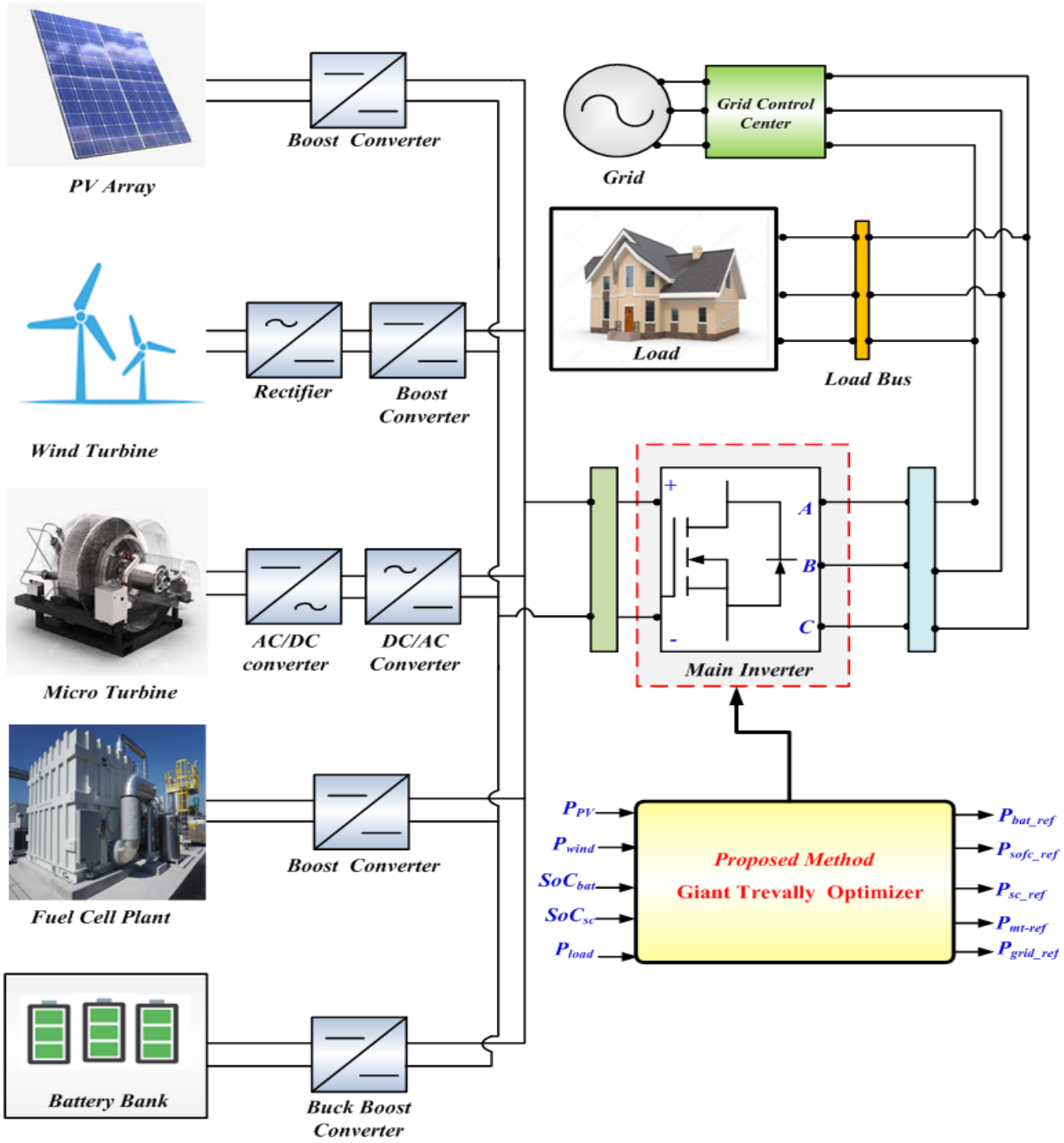


**Fig 1:** Configuration of Renewable Sources Based Micro Grid with Battery Storage System

### 3.1. Modeling of Photovoltaic (PV)

I-V characteristics equation is used to build on the solar cell's mathematical modelling. [28],

$$i = i_{ph} - (i_d - i_{sh}) \quad (1)$$

Where, $i_{ph}$ is represents as source current in (Amps), $i_d$ is denoted as diode current on (Amps), $i_{sh}$ signifies the leakage current in shunt (Amps). Simple output terminal current equation,

$$i = i_{ph} - i_0 \quad (2)$$

Whereas, $i_0$ characterizes the saturation current in (Amps).

$$i_{ph} = \frac{(i_{scr} = K_i \Delta T - i_0)G}{G_r} \quad (3)$$

Whereas, $i_{scr}$ is denoted as represents the rated solar current in ideal weather (25”C and 1000w/m2), $K_i$ represents the temperature of a short circuit, G is a description of the solar irradiation on W/m2, $G_r$ denotes as nominal irradiance under typical meteorological circumstances (25°C and 1000w/m2). $T$ The differences between optimum and recommended temperatures are characteristics of temperature fluctuation. (T-$T_{ref}$ ).

$$_0 = I_{rs}\left(\frac{T}{T_{ref}}\right) 3 \exp\left(\left[\frac{q E_{go}}{ak}\right]\left(\frac{\Delta T}{T_{ref} T}\right)\right) \quad (4)$$

Although, $I_{rs}$ describes the cell's nominal temperature's reverse saturation current and irradiance levels. $E_{go}$ implies energy in the semiconductor band gap.

$$i_{pv} = i_{ph} - i_o\left[\left(\exp\left[\frac{qV_{pv}}{a_{KT}}\right] - 1\right)\right] \quad (5)$$

Source current and Saturation current (Amps) (Amps), $q$ is An essential constant is an electron's charge, indicated by "e." The Boltzmann constant, which is sometimes indicated by the letter "k," is a crucial quantity in thermodynamics that links temperature to the energy of particles in a system. In addition, the diode factor, often known as the ideality factor or n-value, describes how well a diode performs in electrical circuits. To characterize the behavior of electrical components and systems, these characteristics are frequently combined with the operating temperature, expressed in Kelvin, $V_{pv}$ is denoted as each solar voltage is shown.

### 3.2. Modeling of Wind Turbine

The primary source of electricity is a wind turbine (WT), and the amount of electricity it produces is based on the wind's velocity. [29]. Wind speed is broken down into three main categories: cut-in and out speed, rated speed, and overall speed. The rate of change of kinetic energy has a considerable impact on how much WT power is calculated as a consequence.

$$P = \frac{dE}{dt} = \frac{1}{2}\frac{dm_a}{dt}v_W^2 \quad (6)$$

Here, $\frac{dm_a}{dt} = \rho a v_W$ defines the mass flow rate, $a$ specifies the wind area, $\rho$ and specifies air density.

$$P = \frac{1}{2}\rho a v_W^3 \quad (7)$$

The flow of wind energy in both upstream and downstream directions determines the mechanical power that may be extracted, and this connection can be described as follows:

$$P_W = \frac{1}{2}\rho a v_W \left(v_U^2 - v_D^2\right) \quad (8)$$

Here, $v_U$ defines the speed of the wind upstream, $v_D$ denotes the wind speed downstream and the equation above are rewritten as,

$$P_W = \frac{1}{2}\rho a r_p v^3 \quad (9)$$

Where, $P_W$ explains the mechanical force driving the airflow, $r_p$ denotes the power coefficient depends on the ratio of tip speed and the angle of blade pitch.

### 3.3. Modeling of Fuel cell

A fuel cell (FC) transforms chemical energy into electric energy [30]. The FC procedure is identical to the battery process. However, unless supplied with hydrogen and oxygen, FC constantly produces DC electricity. FC is employed in DGS due to its great efficacy, adaptability, and ease of usage. The fuel cell voltage is calculated as follows:

$$v_{FC} = n_{fc}\left[v_0 + \frac{U_g T}{2F}\left(\ln\left(\frac{P_{H_2} P_{O_2}^{1/2}}{P_{H_2O}}\right)\right) - r_i i_{fc}\right] \quad (10)$$

Here, the number of series-connected fuel cells is denoted as $n_{fc}$, We write the standard gas constant as $U_g$, Energy-free voltage is denoted as $v_0$ ,temperature is denoted as $T$, flowing through the stack of fuel cells is denoted as $i_{fc}$ , Faraday constant is denoted as $F$ , the symbols for the partial pressures of oxygen, hydrogen, and water as $P_{H_2}$, $P_{O_2}$, $P_{H_2O}$ respectively.

### 3.5. Modeling of Micro Turbine

The micro turbine, air compressor, and generator of micro-turbines are all connected by a single rotating shaft and rotate at high speeds without lubrication. [31]. The power source is a two-pole, air-cooled permanent magnet generator. This generator propels air into the combustion chamber, where it undergoes compression before being released through the recuperate. By heating entering gases with exhaust gases, the system's efficiency is increased. A power electronic interface is necessary to fill the gap between the micro-turbine and the requirement for AC power. A practical approach involves using the Permanent Magnet Generator (PMG) as the AC power source and modeling a three-phase, full-wave diode bridge rectifier, the generator and rectifier. The inductance precisely represents the equivalent inductance for each generator phase, and losses may be ignored, are our two main presumptions. An ideal Permanent Magnet Generator (PMG) has no load the voltage from line to line, $V_{LL}$ $I$ can be expressed as,

$$V_{LL} = K_v \omega \sin(\omega t) \quad (11)$$

Where, $K_v$ is Particularly in systems utilizing 2-pole Permanent Magnet Generators (PMG), In micro-turbines, the voltage constant and subsequent electrical angular frequency frequently match the mechanical angular frequency. The angular frequency is equal to 9424 radians per second while running at 90,000 RPM. Full-wave rectifiers that maintain a constant current output may be described by the following expression for the DC bus voltage regulation:

$$V_{dc} = \frac{3}{\pi}|V_{LL}| - \frac{3\omega L}{\pi} I_{dc} \quad (12)$$

A funstion of angular frequency and current ,

$$E_g = V_{dc} + K_x \omega I_{dc} \quad (13)$$

Where the open circuit D.C voltage $E_g$ is,

$$E_g = K_e \omega \quad (14)$$

The $K$ is constants are defined as,

$$K_e = \frac{3K_v}{\pi}\{V/(rad/\sec)\} \quad (15)$$

$$K_x = \frac{3L}{\pi\{\Omega/(rad/\sec)\}} \quad (16)$$

To establish the framework for characterizing the electromechanical characteristics of a system, the input power may be expressed when there are no energy losses as a function of $I_{dc}$

$$P_m = V_{dc} I_{dc} = K_e \omega I_{dc} - K_x \omega I_{dc}^2 \quad (17)$$

The mechanical shaft torque for a lossless system can be expressed,

$$Tm = \frac{p_m}{\omega} = K_e I_{dc} - I_{dc}^2 \quad (18)$$

In analyzing the mechanical system, several components need consideration, including the governor, the turbine's response, and the inertia of the shaft (written as J). In this scenario, the governor derives its input from a direct current (D.C.) voltage source. It is presumed that the turbine's reaction can be approximated as a first-order system with time constants typically falling within the range of 5 to 20 seconds.

### 3.6. Mathematical Modeling of Battery System

Battery Energy Storage System (BESS) is displayed in fig 2. These factors have an impact on how much power is generated. Because of their simplicity, durability, and strength—in addition to their commercial viability these batteries are used in the majority of large-scale energy storage projects. Autonomous Days (AD) are commonly used to refer to the period of time during which renewable energy source and battery storage do not conflict with one another in to fulfil load requirement. To Subject AD and the load The following equation serves as the design specification for the battery's capacity,

$$c_b = \frac{(d_l * ad)}{(dod * \eta_{bat} * \eta_{inv})} \quad (19)$$

Where the battery's capacity was indicated as $c_b$, the load demand is indicated as $d_l$, the depth of discharge is signified as $dod$, the effectiveness of the inverter and the battery are indicated as $\eta_{bat}$ and $\eta_{inv}$ respectively. When the hybrid PV/WT system can't provide enough energy, the BESS formulation is employed. To simultaneously increase techno-economic enactment, a hybrid PV/WT and battery system is being designed.

### 3.7. Problem Formulation

Different DERs and battery energy storage solutions are found in micro grids. However, in other cases, the produced electricity might not be sufficient for the micro grid's local need or might be too expensive to be provided by DGs. In this case, micro grids are more effective by acquiring electricity from the local customers with it, or even by storing energy on the power grid. The generating sectors should thus consider the total cost. The whole price may be expressed as,

$$Min\ f(x) = \sum_{t=1}^{T} \cos t^t \quad (20)$$

$$\sum_{t=1}^{T}\left\{\sum_{i=1}^{N_g}\left[U_i(t)p_G(t)B_G(t)+S_G\left|U_i(t)-U_i(t-1)\right|\right]\right\}$$
$$+\sum_{j=1}^{T}[U_j(t)P_{sj}(t)+B_{sj}(t)+S_{sj}\left|U_j(t)-U_j(t-1)\right|] \quad (21)$$
$$+P_{Grid}(t)B_{Grid}(t)U_j(t)$$

Where $X$ and $U_i(t)$ refer to ON/OFF statuses are represented by the state variable vector and state of the $ith$ unit, respectively $B_G$ and $B_{sj}$ represents the bid of $ith$ DG and the $jth$ At the same moment, two storage devices time $t.P_{Grid}$ represents active electricity purchased (sold) from the utility at time $t$ and finally $S_{sj}$ and $S_{G\,show}$ a list of the start-up and ending costs of $jth$ storage system and $ith$ DG, again at time $t$.

$$X=[P_G,U_G]_{1\times 2nT};P_G=[P_G,P_S];\quad n=N_G+N_s+1 \quad (22)$$
$$P_G=[P_G,_1\,P_{G,2},.....P_{G,NG}];\ P_s=[p_{s,1},P_{s,2}....P_{s,N_s}] \quad (23)$$
$$P_{G,i}=[P_G,_1(1)P_{G,2}(2),.....P_{G,i}(T)];\ i=1,2,....N_{G+1} \quad (24)$$
$$P_{S,J}=[P_S,_J(1)P_{S\,J}(2),.....P_{S,J}(T)];\ i=1,2,....N_S \quad (25)$$
$$U_G=[u_1,u_2,....u_n],\qquad u_K\in\{0,1\} \quad (26)$$
$$u_k=[u_K(1),u_K(2),.....u_K(T)];\quad k=1,2,...n \quad (27)$$

$u_K(t)=0\,or\,1$ shows the varying state of the $k_{th}$ unit at time $t$. $N_S$ refers to the quantity of storage devices, while $N_G$ denotes the quantity of power plants.

## 4. Proposed GTO Method Based Micro Grid with Renewable Energy Source

In this paper propose a Giant trevally optimizer (GTO) for the optimal scheduling of a hybrid power system. GTO is used to analyses the generation, storage, and response load options in order to resolve the economic dispatch problems. In the presence of substantial uncertainty, the grid-connected micro grid's optimum energy management is controlled by a GTO algorithm.. The following is a description of the suggested method's thorough justification,

### 4.1. Giant Trevally Optimizer Algorithm

The GTO is a -new swarm-type meta-heuristic algorithm that was developed to optimize a number of significant engineering science issues. It was inspired by the giant trevally's hunting behavior.

***Step 1: Initialization***

Initializing the parameters is the first stage in GTO; in this case, the input parameters are voltage and current.

***Step 2: Random Generation***

GTO represents a possible or workable answer to the optimization problem. Mathematically speaking, each individual in Each of these vectors makes up the algorithm's population matrix, which represents the population as a vector. Equation (28) is used to model the GTO population's members.

$$R=\begin{bmatrix} R_{1,1} & .... & R_{1,j} & .... & R_{1,Dim} \\ R_{i,1} & .... & R_{i,j} & .... & R_{i,Dim} \\ R_{N,1} & .... & R_{N,j} & .... & R_{N,Dim} \end{bmatrix}_{N\times Dim} \quad (28)$$

Here, $R$ implies the potential GTO solution, $X_i$ implies the i[th] potential GTO solution, $Dim$ implies the amount of choice factors in a certain situation, $N$ is how many GTO members , Ri,j is the answer given by the i-th candidate solution for the value of the j-th variable.

***Step 3: Fitness Function***

The evaluation of fitness is based on objective function, which is defined as,

$$F = MIN(\cos t) \tag{29}$$

***Step 4: Extensive Search***

As previously noted, one characteristic of large trevallies is that they are known to travel great distances in quest of their daily food. Consequently, Equation (30) is used in this stage to model the gigantic trevally's foraging movement patterns.

$$X(t+1) = Best_p \times H + ((Max - Min) \times R + Mini) \times Levy(Dim) \tag{30}$$

Here, $X(t+1)$ implies location vector of the following enormous trevally, $Best_p$ indicates the area that gigantic trevallies are now searching for based on the most promising location discovered during their last hunt, $H$ is a number generated at random that ranges from 0 to 1. $Levy(Dim)$ the step sizes of the Levy flight, a certain type of non-Gaussian stochastic processes, named after the Levy distribution,

$$Levy(Dim) = step \times \frac{u \times \sigma}{|v|^{1/\beta}} \tag{31}$$

Where $step$ implies 0.01 step size, $\beta$ is the Levy flight distribution method index vary between 0 to 2 and has a value of 1.5, and $u$ and $v$ implies random values between 0 and 1 with a normal distribution. Equation (6) is used to determine $\sigma$.

$$\sigma = \left( \frac{\Gamma(1+\beta) \times \sin e\left(\frac{\pi\beta}{2}\right)}{\Gamma\left(\frac{1+\beta}{2}\right) \times \beta \times 2\left(\frac{\beta-1}{2}\right)} \right) \tag{32}$$

***Step 5: Choosing Area***

During the stage of picking an area, gigantic trevallies locate and pick the location where they can find the most food (seabirds) inside the chosen search zone. Equation mathematically models this behavior.

$$x(T+1) = Best_p \times a \times r + Mean\_Info - Xi(T) \times r \tag{33}$$

Here, $X(T+1)$ implies enormous trevally position vector in $t$, A is a variable with range that controls position change from 0.3 to 0.4. $Xi(t)$ is the site of the massive travelling company $i$, time $t$. Meanwhile, $Mean\_Info$ relates to the mean shows that all the information from the earlier points has been consumed by these enormous travel falsehoods..

***Step 6: Exploration and Exploitation***

***Exploration:***

The appropriate hunting spot had been found in the stage before, and now, in this phase, which symbolizes the Following its prey bird, the trevally starts the exploitation phase of GTO. When the bird is close enough, the trevally assaults it by leaping out of the water in an aerial attack... Equation (33), which is displayed in the list below, illustrates the Snell's law.

$$\eta_1 \sin\theta_1 = \eta_2 \sin\theta_2 \tag{34}$$

Here $\eta_1$ = 1.00029, $\eta_2$ = 1.33 represents air and water's absolute refractive indices, respectively, whereas $\theta_1$ and $\theta_2$ represents the corresponding angles of incidence and refraction. $\theta_2$ is a random value within the range [0, 360]. From Equation (40), $\theta_1$ can be calculated using below,

$$\sin\theta_1 = \frac{\eta_2}{\eta_1}\sin\theta_2 \quad (35)$$

After that, Equation may be used to compute the visual distortion $\nu$

$$\nu = \sin\left(\theta_1^{\circ}\right)\times D \quad (36)$$

Here, $D$ is the separation between the prey,and attacker, $\sin$ implies $\sin e$ of variable in degrees, and it is measured as

$$D = \left|\left(Best_p - X_i(t)\right)\right| \quad (37)$$

Then, utilizing equation, a gigantic trevally's behavior during a chase and leaping out of the water, which is computed below,

$$X(t+1) = L + \nu + \mathrm{H} \quad (38)$$

Here, $X(T+1)$ implies the outcome of the following iteration $t$, whereby the assaulting step produces. The launch speed $L$ simulates chasing the bird:

$$L = Xi(t)\times\sin(\theta\circ 2)\times F\_obj(Xi(t)) \quad (39)$$

Here $F\_obj(Xi(j))$ implies values of fitness $X$ at iteration $t$.

***Exploitation:***

By employing the previous element in (39) to construct the leaping slope function, the approach may adaptively establish a smooth transition from the research stage to the production stage.

$$\mathrm{H} = R\times(2 - j\times 2T) \quad (40)$$

Where $j$ and $\mathrm{T}$ implies possible iterations and the current iteration, $R$ implies random number, and the various motions felt by the huge trevally throughout the exploitation stage are referenced here. It is important to note that throughout the iteration duration $\mathrm{H}$, has a dropping trend from 2 to 0, and during the exploitation phase,

***Step 7: Termination Criteria***

If the best solution is discovered, check the stopping condition in the termination criteria. The procedure finishes; otherwise, move on to step 3.

**5. Result and Discussion**

In this section outline the performance of proposed approach based on the simulation outcome.. The proposed approach's performance has been assessed within the MATLAB Simulink platform and benchmarked against established methods. The analysis has been conducted using various scheduling methods, including optimal and random schedules. The findings demonstrate that the proposed approach yields a lower cost compared to the existing techniques.

Analysis the power value of proposed (a) PV and (b) Wind is shown in fig 2. Subplot 2(a) shows the power value of PV. The power level initially begins at 0 watts from 0 to 7 hours, gradually increasing until it reaches 370 watts at 0 to 12 hours. Subsequently, the power level decreases to return to 0 watts between 12 and 18 hours. Finally, it maintains a constant power level from 18 to 24 hours. Subplot 2(b) shows the Wind power value. The power initially started at 350W at 2 hours, and then gradually decreased to reach 310W between 2 and 8 hours. Subsequently, there was a slight increase in power, reaching 420W between 8 and 18 hours, followed by a reduction, stabilizing at 370W between 18 and 24 hours. Analysis the power value of proposed (a) MT and Fuel cell is shown in fig 3. Subplot 3(a) shows the MT power value. The power initially started at 140W at 1 hour, and then gradually decreased to reach 110W between 1 and 3 hours. Subsequently, there was a slight increase in power, reaching 150W from 3 to 10 hours. Finally, the power gradually decreased again, ultimately reaching 140W between 10 and 24 hours. Subplot 3(b) shows the fuel cell power value. The power output began at 220 watts at the 2-hour mark, gradually decreasing to 145 watts between the 2nd and 8th hours. Subsequently, there was a slight increase in power, reaching 245 watts from the 8th to the 19th hour, before

declining once again to 210 watts from the 19th to the 24th hour. Analysis the proposed grid power is shown in fig 4. The grid power initially starts at 0 watts and gradually increases to reach 370W between 0 and 8 hours. Subsequently, the power decreases, returning to 0 W between 8 and 13 hours. Afterward, there is a slight increase in power, reaching 170 W between 13 and 15 hours, followed by another reduction, ultimately returning to 0Wbetween 15 and 24 hours. Analysis the power value of BESS is shown in fig 5. The power output commences at 75 kW at the first hour, gradually rising to 320 kW between the first and eighth hours. Subsequently, it decreases, reaching 70 kW over the period spanning from the eighth to the twenty-fourth hour.

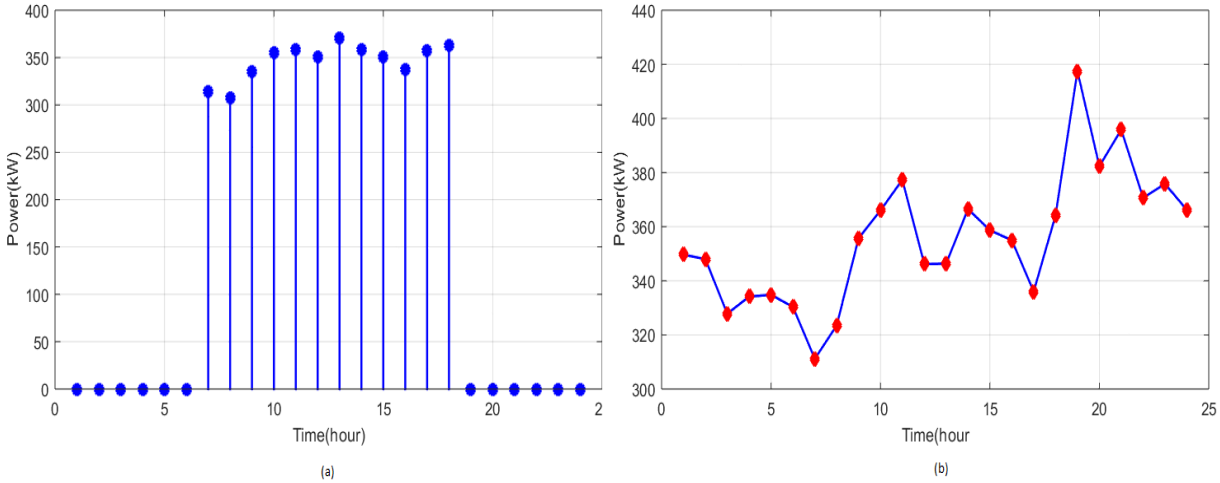


**Fig 2:** Analysis the power value of proposed (a) PV and (b) Wind

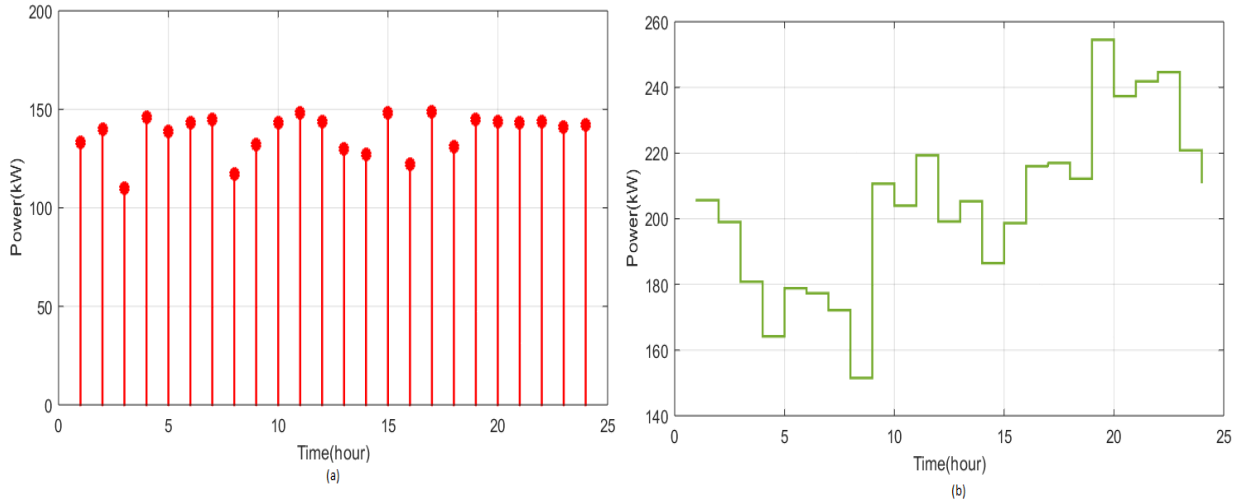


**Fig 3:** Analysis the power value of proposed (a) MT and Fuel cell

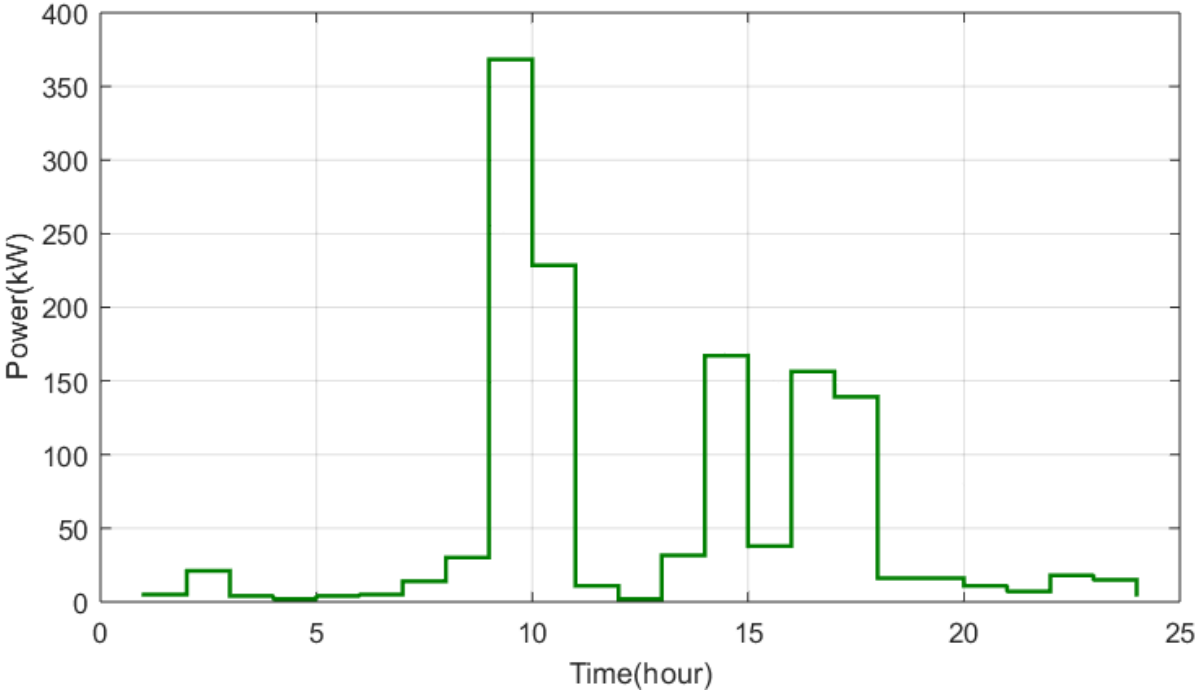


**Fig 4:** Analysis the proposed grid power

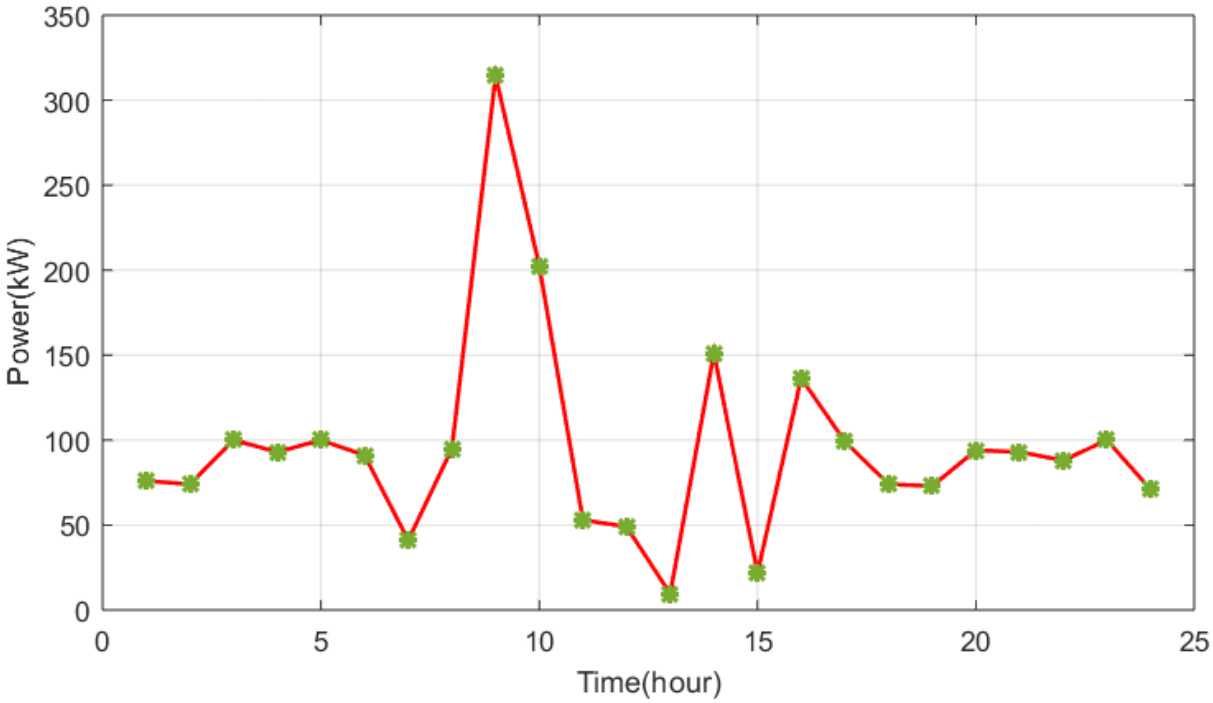


**Fig 5:** Analysis the power value of BESS

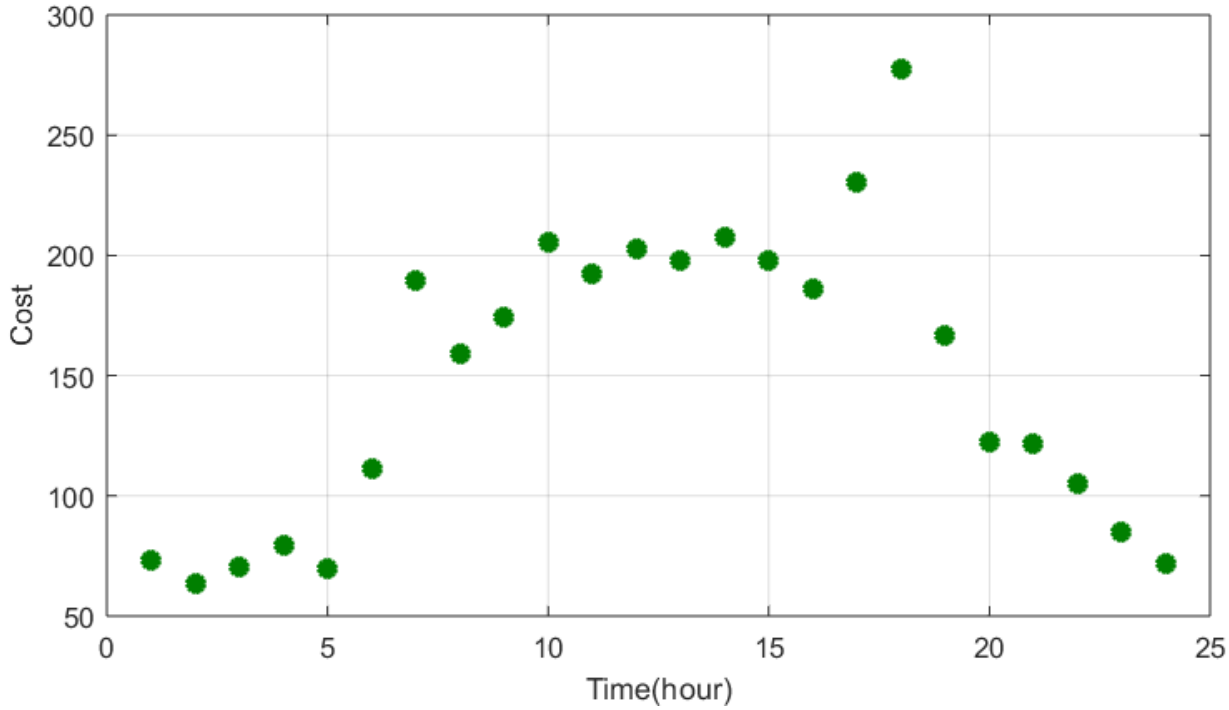


**Fig 6:** Analysis the cost value of proposed method

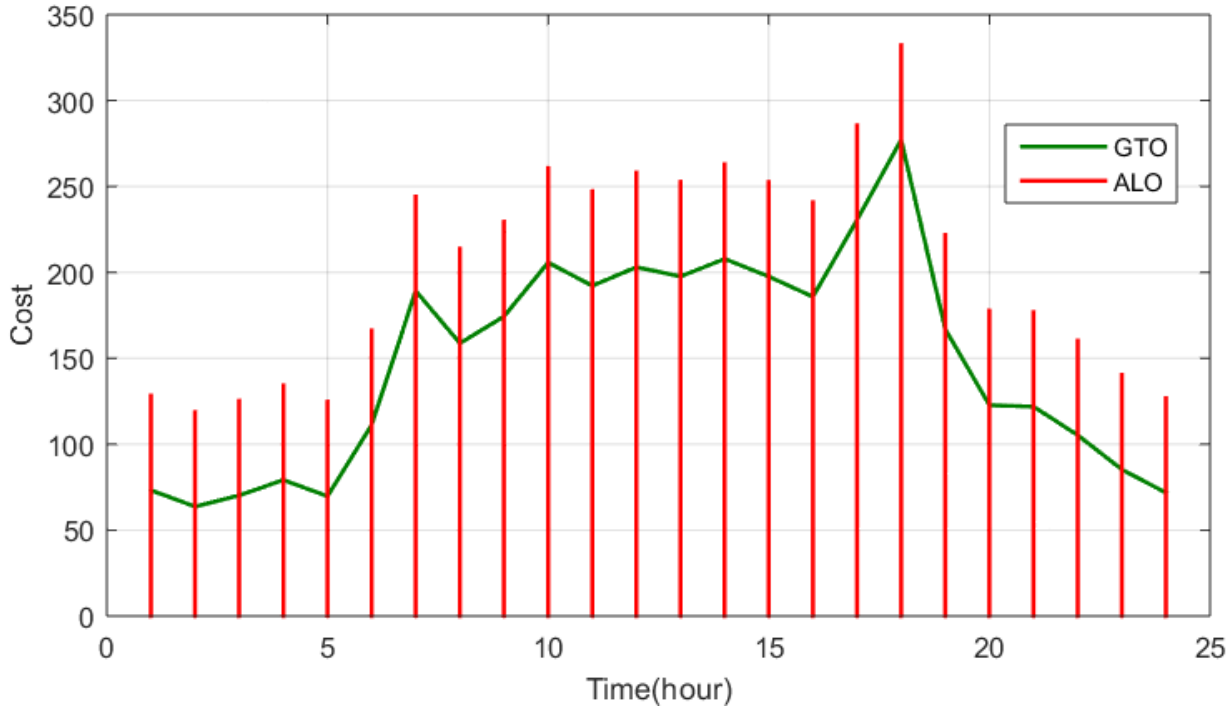


**Fig 7:** Comparison of cost value with proposed and ALO method

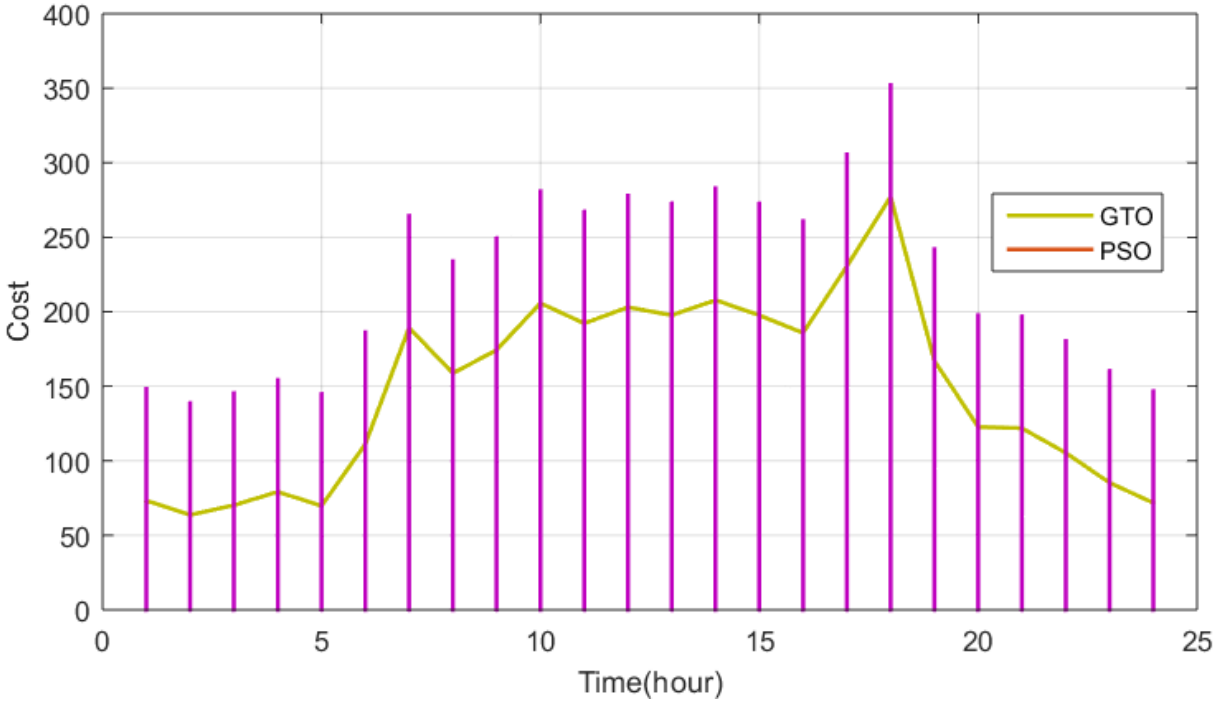


**Fig 8:** Comparison of cost value with proposed and ALO method

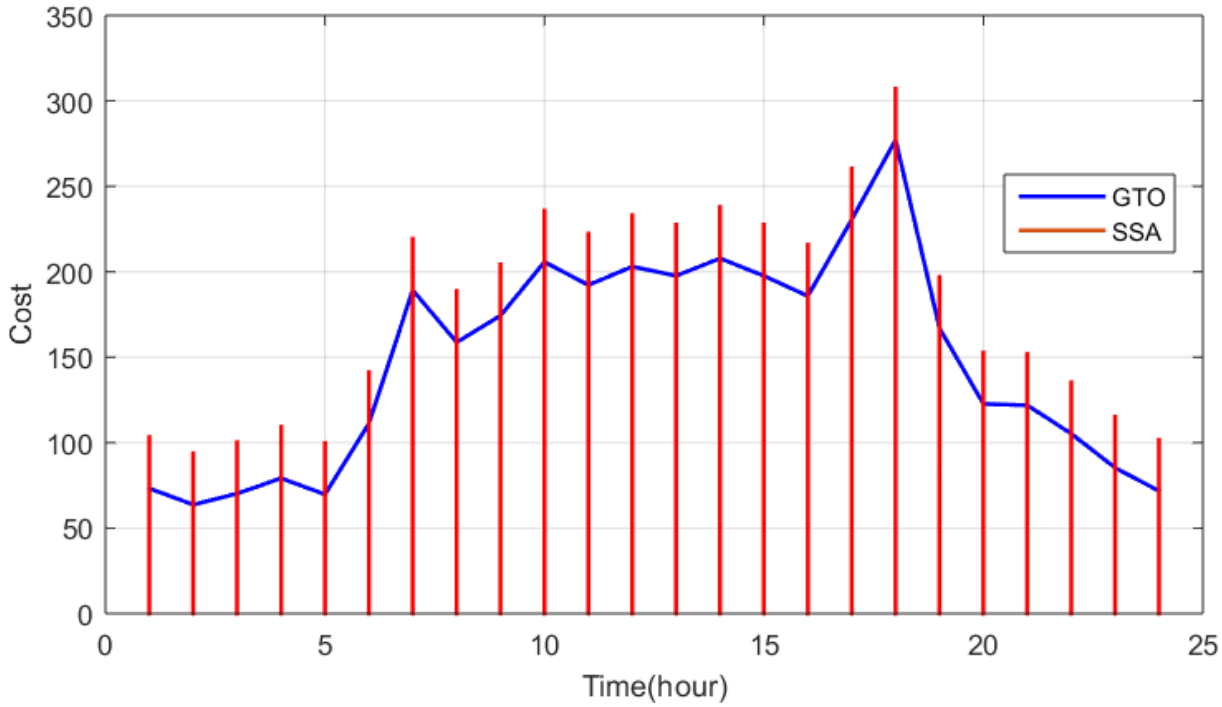


**Fig 9:** Comparison of cost value with proposed and SSA method

---

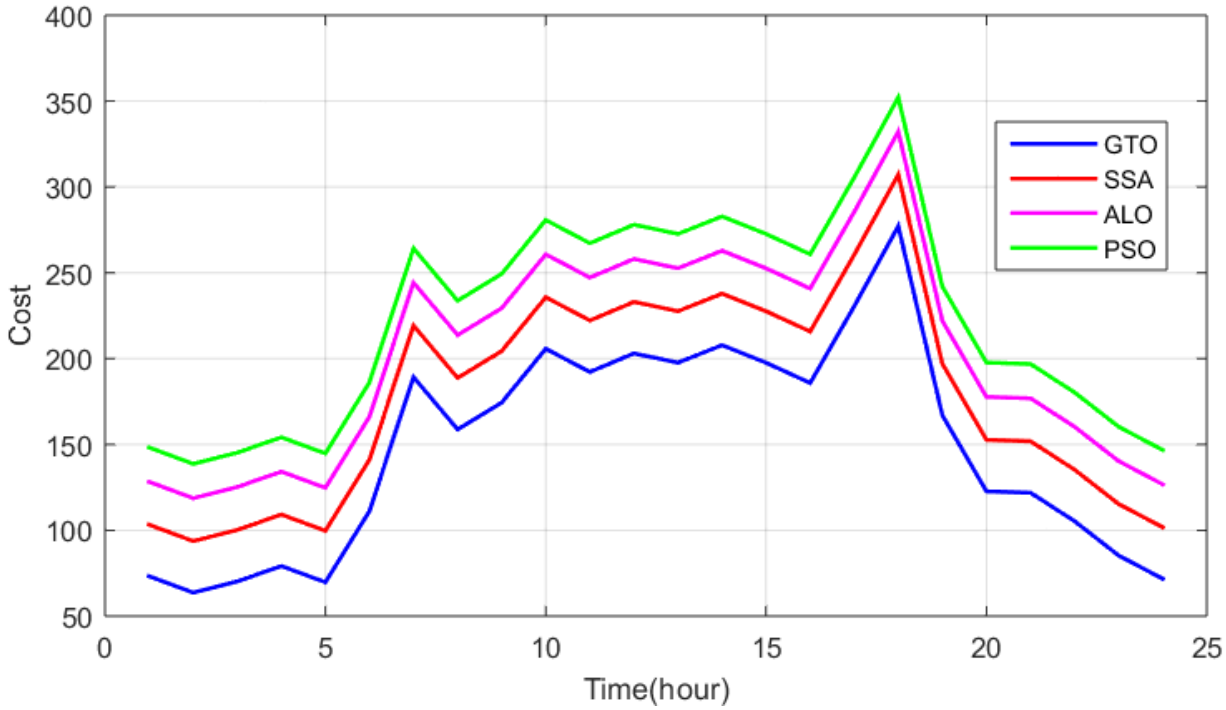


**Fig 10:** Comparison of cost value with proposed and existing methods.

Analysis the cost value of proposed method is shown in fig 6. The initial proposed cost value starts at 75 during the first hour. It then experiences a gradual increase, reaching 270 between the 1st and 17th hours. Subsequently, the cost value decreases, reaching 70 between the 17th and 24th hours. Comparison of cost value with proposed and ALO method is shown in fig 7. The initial cost value for the proposed method begins at 70 at the 1-hour mark. It then experiences a gradual increase, peaking at 270 between 1 and 18 hours. Subsequently, the cost value decreases, returning to 70 between 18 and 24 hours. In contrast, the ALO method starts with an initial cost value of 130 at the 1-hour mark. It follows a similar pattern of gradual increase, reaching a peak of 330 between 1 and 18 hours. Afterward, the cost value decreases, reaching 140 between 18 and 24 hours. Upon comparing the two methods, it is evident that the proposed method consistently maintains a lower cost value than the ALO method. Comparison of cost value with proposed and PSO method is shown in fig 8. The initial cost value for the proposed method begins at 70 during the first hour, gradually rising to 270 over the next 1 to 18 hours. Subsequently, it decreases, reaching 70 again between the 18th and 24th hours. In contrast, the PSO method starts with an initial cost value of 150 in the first hour and experiences a slight increase, reaching 350 between the 1st and 18th hours. It then decreases and returns to 150 between the 18th and 24th hours. Comparatively, the proposed method maintains a lower cost value when compared to the PSO method throughout the entire duration of the analysis. Comparison of cost value with proposed and SSA method is shown in fig 9. The initial cost value of the proposed method starts at 70 at the 1-hour mark, gradually increasing to reach 270 between 1 and 18 hours. Subsequently, it decreases, returning to 70 by the 24-hour mark. In contrast, the cost value of the SSA method commences at 100 at the 1-hour mark, experiences a slight increase, reaching 310 between 1 and 18 hours, and then declines, returning to 100 by the 24-hour mark. It is noteworthy that the proposed method consistently maintains a lower cost value when compared to the SSA method. Comparison of cost value with proposed and existing methods is shown in fig 10. The proposed method exhibits an initial cost value of 70 at the 1-hour mark, which gradually increases to 270 between hours 1 and 18. Subsequently, the cost decreases to 70 from hours 18 to 24. In contrast, the SSA method begins with a cost value of 100 at 1 hour, slightly rising to 310 from hours 1 to 18, before dropping to 100 at hours 18 to 24. When compared, the proposed method consistently demonstrates lower cost values than the SSA method. Similarly, the ALO method initiates with a cost value of 130 at 1 hour, experiences a slight increase to 330 between hours

1 and 18, and then reduces to 140 from hours 18 to 24. In this case, the proposed method also outperforms the ALO method by maintaining a lower cost. Lastly, the PSO method starts with a cost value of 150 at 1 hour, undergoes a slight increase to 350 between hours 1 and 18, and eventually drops to 150 from hours 18 to 24. Once again, the proposed method consistently exhibits a lower cost compared to the PSO method. As a result, it can be said that when compared to other current approaches, the suggested method consistently exhibits higher cost performance.

**Table 1:** Analysis of Proposed and Exiting Methods cost value with one day

| Methods | Cost ($) | | | | |
|---|---|---|---|---|---|
| | 0 to 5 (hour) | 5 to 10 (hour) | 10 to 15 (hour) | 15 to 20 (hour) | 20 to 24 (hour) |
| PSO | 150 | 270 | 265 | 360 | 150 |
| ALO | 140 | 260 | 250 | 340 | 130 |
| SSA | 100 | 230 | 230 | 320 | 100 |
| GTO | 70 | 210 | 200 | 280 | 70 |

Analysis of Proposed and Exiting Methods cost value with one day is shown in table 1. The proposed method cost value is lower than other existing methods.

## 5. Conclusion

This study suggests employing Optimal Scheduling of Renewable Sources Based Micro grid with PV and Battery Storage Using Giant Trevally Optimizer" presents a comprehensive analysis of an innovative approach to managing renewable energy resources within a micro grid Micro grid operators may improve the dependability and resilience of their systems by utilizing GTO, The proposed method is evaluated in the MATLAB Simulink platform and contrasted with different other methods already in use. The goal is to optimize the energy management system in order to decrease the overall operational expenses of the grid-connected micro grid. The results also indicate that the proposed method significantly outperforms other optimization techniques. The proposed method cost value is 270 is lower than other existing methods.

## Reference

[1] Jabari, F., Arasteh, H., Sheikhi-Fini, A., Ghaebi, H., Bannae-Sharifian, M. B., Mohammadi-Ivatloo, B., & Mohammadpourfard, M. (2022). A biogas-steam combined cycle for sustainable development of industrial-scale water-power hybrid microgrids: design and optimal scheduling. Biofuels, Bioproducts and Biorefining, 16(1), 172-192.

[2] Mao, A., Yu, T., Ding, Z., Fang, S., Guo, J., & Sheng, Q. (2022). Optimal scheduling for seaport integrated energy system considering flexible berth allocation. Applied Energy, 308, 118386.

[3] Cheng, Z., Jia, D., Li, Z., Si, J., & Xu, S. (2022). Multi-time scale dynamic robust optimal scheduling of CCHP microgrid based on rolling optimization. International Journal of Electrical Power & Energy Systems, 139, 107957.

[4] Komeili, M., Nazarian, P., Safari, A., & Moradlou, M. (2022). Robust optimal scheduling of CHP-based microgrids in presence of wind and photovoltaic generation units: An IGDT approach. Sustainable Cities and Society, 78, 103566.

[5] Cao, Y., Huang, L., Li, Y., Jermsittiparsert, K., Ahmadi-Nezamabad, H., & Nojavan, S. (2020). Optimal scheduling of electric vehicles aggregator under market price uncertainty using robust optimization technique. International Journal of Electrical Power & Energy Systems, 117, 105628.

[6] Li, Y., Wang, B., Yang, Z., Li, J., & Li, G. (2021). Optimal scheduling of integrated demand response-enabled community-integrated energy systems in uncertain environments. IEEE Transactions on Industry Applications, 58(2), 2640-2651.

[7] Luo, L., Abdulkareem, S. S., Rezvani, A., Miveh, M. R., Samad, S., Aljojo, N., & Pazhoohesh, M. (2020). Optimal scheduling of a renewable based microgrid considering photovoltaic system and battery energy storage under uncertainty. Journal of Energy Storage, 28, 101306.

[8] Li, Y., Li, K., Yang, Z., Yu, Y., Xu, R., & Yang, M. (2022). Stochastic optimal scheduling of demand response-enabled microgrids with renewable generations: An analytical-heuristic approach. Journal of Cleaner Production, 330, 129840.

[9] Zhu, X., Yang, J., Liu, Y., Liu, C., Miao, B., & Chen, L. (2019). Optimal scheduling method for a regional integrated energy system considering joint virtual energy storage. Ieee Access, 7, 138260-138272.

[10] Bostan, A., Nazar, M. S., Shafie-Khah, M., & Catalão, J. P. (2020). Optimal scheduling of distribution systems considering multiple downward energy hubs and demand response programs. Energy, 190, 116349.

[11] Li, Y., Wang, C., Li, G., & Chen, C. (2021). Optimal scheduling of integrated demand response-enabled integrated energy systems with uncertain renewable generations: A Stackelberg game approach. Energy Conversion and Management, 235, 113996.

[12] Huang, X., Zhang, Y., Li, D., & Han, L. (2019). An optimal scheduling algorithm for hybrid EV charging scenario using consortium blockchains. Future Generation Computer Systems, 91, 555-562.

[13] Emrani-Rahaghi, P., & Hashemi-Dezaki, H. (2021). Optimal scenario-based operation and scheduling of residential energy hubs including plug-in hybrid electric vehicle and heat storage system considering the uncertainties of electricity price and renewable distributed generations. Journal of Energy Storage, 33, 102038.

[14] Hein, K., Xu, Y., Wilson, G., & Gupta, A. K. (2020). Coordinated optimal voyage planning and energy management of all-electric ship with hybrid energy storage system. IEEE Transactions on Power Systems, 36(3), 2355-2365.

[15] Wang, Y., Zhao, M., Chang, J., Wang, X., & Tian, Y. (2019). Study on the combined operation of a hydro-thermal-wind hybrid power system based on hydro-wind power compensating principles. Energy Conversion and Management, 194, 94-111.

[16] Moghaddas-Tafreshi, S. M., Mohseni, S., Karami, M. E., & Kelly, S. (2019). Optimal energy management of a grid-connected multiple energy carrier micro-grid. Applied Thermal Engineering, 152, 796-806.

[17] Nasiri, N., Zeynali, S., Ravadanegh, S. N., & Marzband, M. (2021). A hybrid robust-stochastic approach for strategic scheduling of a multi-energy system as a price-maker player in day-ahead wholesale market. Energy, 235, 121398.

[18] Alahyari, A., Ehsan, M., & Mousavizadeh, M. (2019). A hybrid storage-wind virtual power plant (VPP) participation in the electricity markets: A self-scheduling optimization considering price, renewable generation, and electric vehicles uncertainties. Journal of Energy Storage, 25, 100812.

[19] Liu, C., Abdulkareem, S. S., Rezvani, A., Samad, S., Aljojo, N., Foong, L. K., & Nishihara, K. (2020). Stochastic scheduling of a renewable-based microgrid in the presence of electric vehicles using modified harmony search algorithm with control policies. Sustainable cities and society, 59, 102183.

[20] Zhang, G., Hu, W., Cao, D., Liu, W., Huang, R., Huang, Q., ... & Blaabjerg, F. (2021). Data-driven optimal energy management for a wind-solar-diesel-battery-reverse osmosis hybrid energy system using a deep reinforcement learning approach. Energy conversion and management, 227, 113608.

[21] Eskandari, H., Kiani, M., Zadehbagheri, M., & Niknam, T. (2022). Optimal scheduling of storage device, renewable resources and hydrogen storage in combined heat and power microgrids in the presence plug-in hybrid electric vehicles and their charging demand. Journal of Energy Storage, 50, 104558.

[22] Wang, H., Xing, H., Luo, Y., & Zhang, W. (2023). Optimal scheduling of micro-energy grid with integrated demand response based on chance-constrained programming. International Journal of Electrical Power & Energy Systems, 144, 108602.

[23] Li, Y., Bu, F., Li, Y., & Long, C. (2023). Optimal scheduling of island integrated energy systems considering multi-uncertainties and hydrothermal simultaneous transmission: A deep reinforcement learning approach. Applied Energy, 333, 120540.

[24] Alabi, T. M., Lu, L., & Yang, Z. (2022). Data-driven optimal scheduling of multi-energy system virtual power plant (MEVPP) incorporating carbon capture system (CCS), electric vehicle flexibility, and clean energy marketer (CEM) strategy. Applied Energy, 314, 118997.

[25] Dey, B., Raj, S., Mahapatra, S., & Márquez, F. P. G. (2022). Optimal scheduling of distributed energy resources in microgrid systems based on electricity market pricing strategies by a novel hybrid optimization technique. International Journal of Electrical Power & Energy Systems, 134, 107419.

[26] Zakernezhad, H., Nazar, M. S., Shafie-khah, M., & Catalao, J. P. (2022). Optimal scheduling of an active distribution system considering distributed energy resources, demand response aggregators and electrical energy storage. Applied Energy, 314, 118865.

[27] Yang, P., Jiang, H., Liu, C., Kang, L., & Wang, C. (2023). Coordinated optimization scheduling operation of integrated energy system considering demand response and carbon trading mechanism. International Journal of Electrical Power & Energy Systems, 147, 108902.

[28] Mayer, M. J., & Gróf, G. (2021). Extensive comparison of physical models for photovoltaic power forecasting. Applied Energy, 283, 116239.

[29] Ti, Z., Deng, X. W., & Yang, H. (2020). Wake modeling of wind turbines using machine learning. Applied Energy, 257, 114025.

[30] Cao, Y., Li, Y., Zhang, G., Jermsittiparsert, K., & Razmjooy, N. (2019). Experimental modeling of PEM fuel cells using a new improved seagull optimization algorithm. Energy Reports, 5, 1616-1625.

[31] Abd El-Sattar, H., Kamel, S., Tawfik, M. A., Vera, D., & Jurado, F. (2019). Modeling and simulation of corn stover gasifier and micro-turbine for power generation. Waste and Biomass Valorization, 10, 3101-3114.

[32] Calero, F., Cañizares, C. A., & Bhattacharya, K. (2020). Dynamic modeling of battery energy storage and applications in transmission systems. IEEE Transactions on Smart Grid, 12(1), 589-598.

[33] adeeq, H. T., & Abdulazeez, A. M. (2022). Giant trevally optimizer (GTO): A novel metaheuristic algorithm for global optimization and challenging engineering problems. IEEE Access, 10, 121615-121640.

[34] Kabat, S. R., Panigrahi, C. K., Ganthia, B. P., Barik, S. K., & Nayak, B. (2022). Implementation and analysis of mathematical modeled drive train system in type III wind turbines using computational fluid dynamics. Advances in Science and Technology. Research Journal, 16(1), 180-189.